

PLA-90-59

90/08/31

1 GeV リニアック検討資料

1 GEV LINAC DESIGN NOTE

題目(TITLE)

A HIGH-POWER MODEL OF THE ACS
CAVITY

著者(AUTHOR)

T. Kageyama, Y. Morozumi, Y. Yamazaki, and K. Yoshino

概要(ABSTRACT)

During the last two years, we have developed four-slot Annular Coupled Structure (ACS) for the high- β coupled-cell linac used for the 1-GeV proton linac of the Japanese Hadron Project (JHP). In order to study the performance in high-power operation, a 1296-MHz high-power mode of the four-slot ACS has been designed and constructed. The cavity has been successfully conditioned up to the designed value. This report presents the cavity design, thermal analysis for optimizing the cooling-water circuits, the RF properties, and the results of the high-power test.

KEY WORDS: Ion Source, RFQ, DTL, CCL, Magnet, Monitor, Beam Dynamics, Transport, Vacuum, Cooling, Klystron, Low Level RF, High Power RF, Modulator, Control, Operation, Radiation, Others

高エネルギー物理学研究所 KEK

A HIGH-POWER MODEL OF THE ACS CAVITY

T. Kageyama, Y. Morozumi, Y. Yamazaki, and K. Yoshino

KEK, National Laboratory for High Energy Physics, Oho 1-1, Tsukuba-shi, Ibaraki-ken 305, Japan

Abstract

During the last two years, we have developed the four-slot Annular Coupled Structure (ACS) for the high- β coupled-cell linac used for the 1-GeV proton linac of the Japanese Hadron Project (JHP). In order to study the performance in high-power operation, a 1296-MHz high-power model of the four-slot ACS cavity has been designed and constructed. The cavity has been successfully conditioned up to the designed value. This report presents the cavity design, thermal analysis for optimizing the cooling-water circuits, the RF properties, and the results of the high-power test.

Introduction

The standing-wave $\pi/2$ -mode operation of a chain of coupled cavities has advantages over the π -mode operation; 1) a high degree of cell-to-cell uniformity in the accelerating field against cell-to-cell frequency errors, 2) a high degree of stability in the accelerating field between cells against turbulence by heavy beam loading.

For a $\pi/2$ -mode coupled-cell structure, accelerating cells are located alternately with non-excited coupling cells. A disk-loaded structure operated in the $\pi/2$ mode¹ is a simple example; it is referred to as On-axis Coupled Structure (OCS). However, for the OCS, the shunt impedance is reduced owing to the coupling cells located on the beam axis. The side-coupled structure² was invented in order to avoid this loss by placing the coupling cell at the side of the accelerating cell, that is, off from the beam axis. Another possibility is the Annular Coupled Structure (ACS), which has an annular coupling cell around the accelerating cell instead of a pillbox-type cell.

Although several studies^{3,4,5} using cold models have been made, no ACS cavities have been developed up to the level for practical use. Difficulties in developing ACS cavities arise from RF properties of the annular coupling cell; the annular cell has the higher order modes of TM_{110} and TM_{210} in the neighborhood above the coupling mode of TM_{010} .

The previous studies^{4,5} on the ACS (with two coupling slots between the accelerating and annular coupling cells) can be summarized as follows. 1) When the slots face each other with respect to the central symmetrical plane of the annular cell (cell-to-cell slot orientation = 0°), the TM_{110} mode intrudes into the accelerating passband as the coupling factor increases. 2) When the cell-to-cell slot orientation is 90° , the accelerating mode excites a TM_{210} -like mode in the annular cell, resulting in the reduction in the shunt impedance.

Development of Multi-slot ACS

We have studied on the two-slot ACS by using the computer code MAFIA⁶, and obtained the following results⁷. 1) The difficulties regarding the two-slot ACS arises from the breakdown in the axial symmetry by opening two slots. Compared with the mode spacings among the TM_{010} , TM_{110} and TM_{210} modes, the degree of breakdown is not small, resulting in perturbative effects such as mode mixing. 2) The difficulties can be cured by increasing the number of slots (multi-slot configuration) and reducing the size of each slot, that is, by recovering the axial symmetry.

In order to study the possibility of the multi-slot ACS, we have made 4-slot and 8-slot cold models and measured their RF properties. From the measurements, we have obtained the following results⁷: 1) the difficulties regarding 2-slot ACS are cured by 4-slot configurations with cell-to-cell orientation = 0° and 45° ; 2) no improvements were observed by increasing the number of slots from 4 to 8. As the number of coupling slots increases, the structural strength of the cavity

becomes inferior. Therefore, the 4-slot ACS is probably one of the most practical choices.

According to the measurement of a 4-slot ACS model cavity with a coupling factor of 0.05, the effective shunt impedance has been reduced by 20% owing to the effect of coupling slots and by 5% owing to the surface imperfection. Since the 4-slot ACS is more advantageous than the SCS regarding its axial symmetry, we start the design and construction of a high-power model of the 4-slot ACS (cell-to-cell orientation = 45°) in the summer of 1989.

High-Power Model

Overall Design

As shown in Fig. 1 and 2, the high-power model comprises a pair of ACS cavities coupled via a bridge coupler. It is designed as a prototype for the coupled-cell accelerating structure at $\beta=0.78$ of the

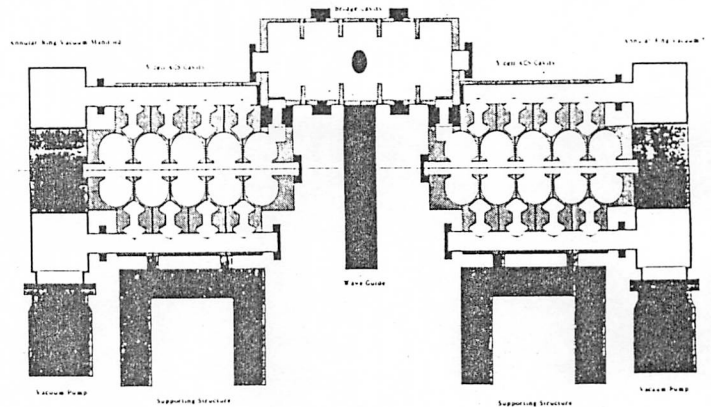


Fig. 1. A schematic drawing of the high-power model.

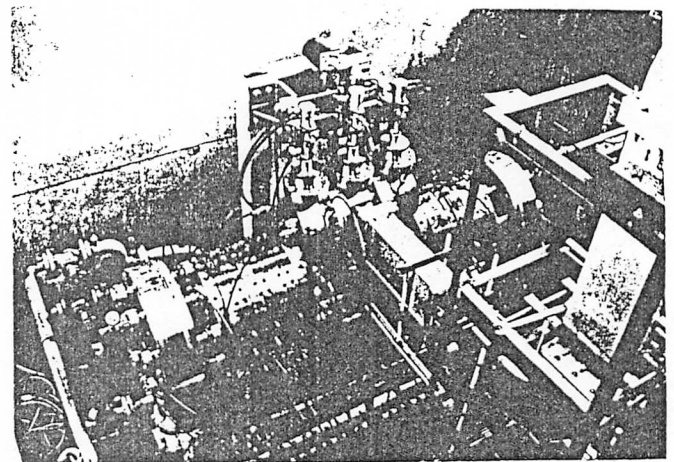


Fig. 2. The high-power model with waveguide in the test bench.

JHP 1-GeV proton linac. Design parameters for the high-power model are listed in Table 1. The shunt impedance and Q values in Table 1 are those calculated by SUPERFISH⁸, which does not include the effect of coupling slots. For each ACS cavity-unit, five accelerating cells are arranged alternately with four annular coupling cells. For the bridge coupler, it was designed to be a 5-cell disk-loaded structure in order to avoid the mode-mixing between the TM_{01} and TE_{11} modes in a long cylindrical cavity. The ACS cavity and the bridge coupler is electromagnetically coupled via a side-coupled pillbox cavity. The RF power is fed through the iris at the central cell of the bridge coupler. Details on the disk-loaded bridge coupler are described in Ref. 9.

In order to generate the designed accelerating gradient of 4.5 MV/m, a peak RF power of 27 kW is required, considering the reduction of 20~25% in the shunt impedance compared with the theoretical value. Including the wall loss in the bridge coupler, the high-power model requires a peak RF power of 300 kW in total.

TABLE 1
Design Parameters for the ACS High-Power Model ($\beta=0.78$)

frequency	1296	MHz
accelerating gradient	4.5	MV/m
shunt impedance	54	$M\Omega/m$
transit time factor	0.80	
Q value of accelerating cell	2.4×10^4	
Q value of coupling cell	9.6×10^3	
peak RF power per cell *	27	kW

* using the effective shunt impedance (80% of the theoretical value)

Structure of the ACS Cavity

The ACS cavity is a brazed assembly of eight middle segments and two end segments (Fig. 1). All the segments were machined from oxygen-free copper (OFC) by a super-precision lathe, and assembled by vacuum-furnace brazing. Further particulars on the fabrication techniques are found in Ref. 10.

Figure 3 shows the middle segment. The shape of the accelerating cell was optimized for the shunt impedance by using the computer code SUPERFISH⁸. The annular coupling cell is like a resonant ring of ridged-waveguide. The cross-sectional shape of ridged-waveguide was adjusted in order to make the diameter of the annular cell as small as possible. Four coupling slots are bored through the septum between the accelerating and annular coupling cells. According to the thermal analysis described later, a minimum septum thickness of 10 mm is required in order to drill cooling-water channels in it. Therefore, we refined the design of the coupling slot bored through the 10-mm-thick

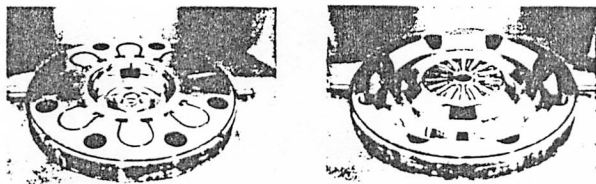


Fig. 3. Middle segment of the high-power model of the ACS cavity. The accelerating-cell side is shown in the left and the annular coupling-cell side in the right.

septum. In order to make both the magnetic coupling efficient and the arc-length of the slot as small as possible, both radial sides of the slot were taper-edged. The slot size was determined to be 32.5° in arc length and 26 mm in radial length by measurement of half-scale models.

The middle-segment have eight circular holes around the annular cell (Fig. 3). When all the segments are stacked and brazed, these holes form pumping-out ports running through the ACS cavity in the longitudinal direction. An annular vacuum manifold is attached to the end of each ACS cavity (Fig. 1 and 2).

Thermal Analysis

The time-averaged power dissipation amounts to about 1 kW per accelerating cell as can be seen in Table 1. In order to make the thermal detuning as small as possible under high-duty operation, we have optimized the arrangement of cooling-water circuits by carrying out both thermal and structural finite element analyses for two-dimensional and three-dimensional structures by the computer code of Integrated Structure Analysis System (ISAS2)¹¹. The thermal analysis indicates that the temperature rise at the nose cone amounts to 35°C with circumferential cooling circuits only, giving rise to a too large frequency detuning of about -510 kHz. This is due to the poor thermal conductivity at the septum between the accelerating and annular coupling cells, where four coupling slots are bored. Therefore, the nose cone region must be cooled directly by water flowing in the disk. Figure 4 shows the final design of cooling circuits, which requires channels drilled in the septum for water inlets and outlets. The temperature rise at the nose cone was drastically reduced to 3.1°C with 5 l/min of cooling water per disk, resulting in a detuning of -110 kHz.

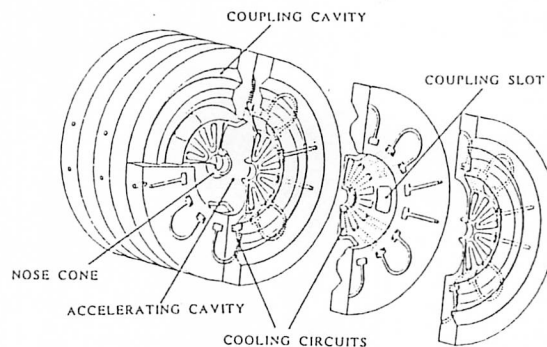


Fig. 4. Cooling-Water Circuits for the high-power model.

RF Properties

Prior to brazing, individual cells were tuned to the design frequency within ± 100 kHz by fine machining. For the accelerating cell, either the nose cone or the inner surface along the line of latitude was machined. For the annular coupling cell, the height of the ridge was adjusted by fine machining. After brazing, if necessary, individual cells can be tuned by dimpling the thin-wall parts from outside.

Since the segments made of OFC are soft and easily deformed, we can not press stacked cavity-segments until its Q value is saturated, without causing considerable deformation. Therefore, the reduction in the Q value due to the surface imperfection was estimated from the result of a half-scale single-cell cavity ($f = 2600$ MHz), the inner surface of which was machined under the same condition as the high-

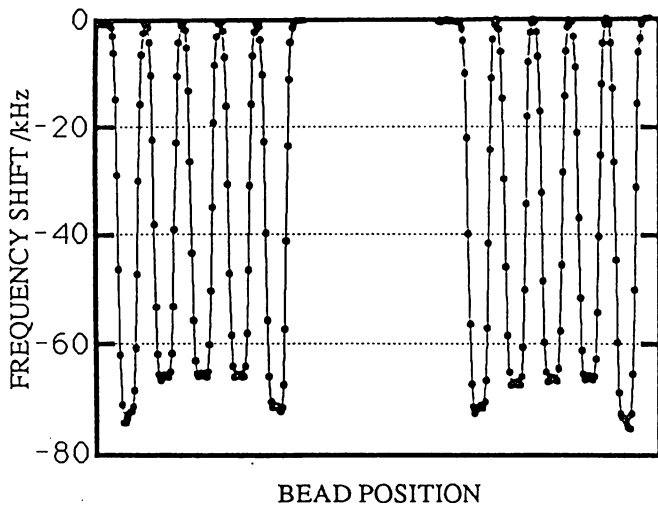


Fig. 5. A distribution of the accelerating field on the beam axis obtained by bead-perturbation measurement.

power model. The measured Q value was small by 4% compared with the theoretical value. Considering the skin-depth dependence on the RF frequency, the reduction for the high-power model ($f = 1296$ MHz) should be less than 4%.

The coupling factor was measured for all the middle-segment pairs stacked with cell-to-cell orientation = 45° . The result of $k = 0.0551 \pm 0.0002$ indicates that the high accuracy was kept with a numerically controlled cutter during machining all the coupling slots.

After the construction at the MHI Mihara Works¹⁰ completed, several low-level measurements were carried out at the high-power test bench in KEK. With a waveguide duct and an RF window, the loaded Q value and the coupling β of the high-power model were measured to be 9.8×10^3 and 0.98, respectively, indicating that the unloaded Q value was 1.9×10^4 . The stored energy in the bridge coupler is 7.1% of the total⁷, and its theoretical Q value is 2.5×10^4 . Therefore, within an error of 1%, the Q value of the ACS cavity itself should be 1.9×10^4 , which is small by 21% compared with the theoretical value. Supposing a reduction of 4% arises from the surface imperfection, the rest of 17% should be due to the effect of the coupling slots.

The accelerating-field distribution on the beam axis was measured by using the bead-perturbation technique. It can be seen from Fig. 5 that the obtained field distribution was sufficiently uniform. Thus, we decided to make no tuning of individual cells by dimpling the thin-wall parts. Since the gap length of the middle-cell was enlarged by 5% compared with that of the end-cell in order to compensate a frequency decrease by the coupling slots, the electric field in the end-cell is larger than that in the middle cell by 4~5%.

From the field distribution data for a middle-cell, the R/Q value was calculated to be $201 \Omega/\text{cell}$. This value is in good agreement with the theoretical value of $205 \Omega/\text{cell}$ by SUPERFISH⁸. Using the Q and R/Q values obtained from the measurements, the effective shunt impedance was estimated to be $42 \text{ M}\Omega/\text{m}$. The reduction in the shunt impedance is 22% compared with the theoretical value, reflecting only the reduction in the Q value.

High-Power Test

The first RF conditioning was carried out at a low duty factor of 0.2%, where RF pulses were 200- μs duration at 10 Hz. The cavity was evacuated by two 300-l/s turbo-molecular pumps attached to the vacuum manifolds at both ends. The base pressure was 1.5×10^{-7} Torr when the RF off. Keeping the vacuum level below 2×10^{-6} Torr, the conditioning was progressed continuously. Through a pumping-out port, the annular coupling cells were monitored by a TV camera.

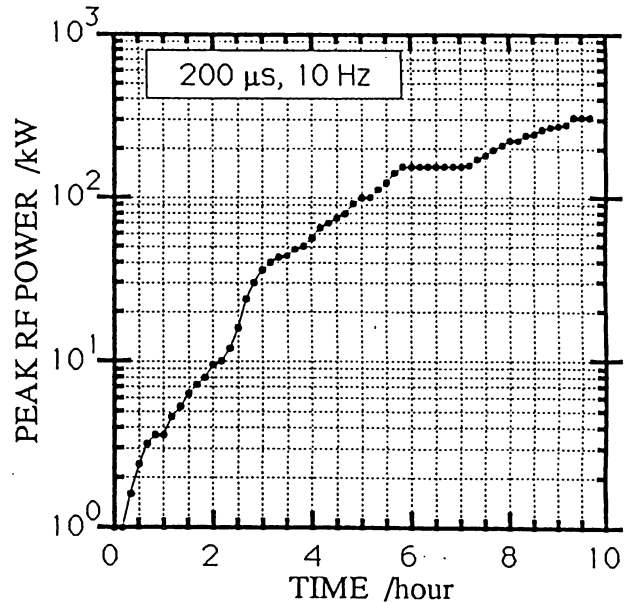


Fig. 6. The history of the first conditioning at a duty factor of 0.2% (200 μs , 10 Hz).

During conditioning, no light emissions due to electric discharge or arcing were observed. Figure 6 shows the history of the first conditioning. The plateau of the history curve at 170 kW is probably the conditioning of the RF window. In proceeding on the plateau, blue light emissions were often observed around the RF window through a TV camera. The cavity was conditioned up to the design RF power level of 300 kW in 10 hours. After the conditioning, the base pressure was improved down to 1.2×10^{-7} Torr.

Conclusions

The high-power model of the 4-slot ACS cavity has been developed. The effective shunt impedance was 78% of the theoretical value. Without tuning of individual cells after brazing, a sufficiently uniform accelerating-field distribution has been obtained. The model has been successfully conditioned up to the design RF power level of 300 kW.

The RF conditioning will be carried out at the full duty factor of 3% in the near future, where the RF pulses are 600- μs duration at 50 Hz. The design of a ACS cavity for a low β of 0.5 is also in progress.

References

1. T. Nishikawa, S. Giordano, and D. Carter, *Rev. Sci. Instr.* 37, 652 (1966).
2. E.A. Knapp, B.C. Knapp, and J.M. Potter, *Rev. Sci. Instr.* 39, 979 (1968)
3. V.G. Andreev et al., *Proc. Proton Linac Conf.*, 114 (1972)
4. R.K. Cooper et al., *Preprint LA-UR-83-95* (Los Alamos National Laboratory) (1983)
5. R.A. Hoffswell and R.M. Laszewski, *IEEE Trans. on Nucl. Sci.* 30, 3588 (1983)
6. T. Weiland, *Part. Accel.* 17, 227 (1985)
7. T. Kageyama et al., *Part. Accel.* 32, 33 (1990)
8. K. Habach and R.F. Holsinger, *Part. Accel.* 7, 213 (1976)
9. Y. Morozumi et al., "Multi-Cavity Bridge Coupler," this conference
10. K. Yamasu et al., "Fabrication Technique of ACS Cavity," this conference
11. ISAS2 is a software by Hitachi, Ltd.